Available online at www.sciencedirect.com
SCIENCE DIRECT
Journal of Catalysis 234 (2005) 230–239
JOURNAL OF CATALYSIS
www.elsevier.com/locate/jcat

Enantioselectivity and catalyst morphology: step and terrace site contributions to rate and enantiomeric excess in Pt-catalysed ethyl pyruvate hydrogenation

D.J. Jenkins [a], A.M.S. Alabdulrahman [a], G.A. Attard [a,*], K.G. Griffin [b], P. Johnston [b], P.B. Wells [a,*]

[a] *School of Chemistry, Cardiff University, Museum Avenue, Cardiff, CF10 3AT, UK*
[b] *Johnson Matthey, Orchard Road, Royston, Herts, SG8 5HE, UK*

Received 5 May 2005; revised 16 June 2005; accepted 20 June 2005

Available online 21 July 2005

Abstract

The steps (Pt{111} × {111} and Pt{100} × {111}) and terraces (Pt{100} and Pt{111}) of a 5% Pt/graphite catalyst have been identified by cyclic voltammetry and their contributions to rate and enantioselectivity in high-pressure ethyl pyruvate hydrogenation assessed. Bi preferentially adsorbed from solution onto the platinum surface of the catalyst at step and {100} terrace sites. Further increasing Bi coverage led to the gradual occupation of {111} terrace sites, followed by the formation of Bi multilayers. In contrast, S adsorbed from solution onto terrace and step sites simultaneously but with the {111} × {111} step sites being strongly disfavoured. Pt/graphite, Bi–Pt/graphite, and S–Pt/graphite catalysts have been modified by cinchonidine and used to catalyse the enantioselective hydrogenation of ethyl pyruvate to ethyl lactate at 30 bar and 293 K. The effect of increasing Bi coverage at step sites was to increase activity substantially but reduce enantiomeric excess from 43%(R) to 17%(R), whereas the effect of increasing S adsorption at terrace sites was to decrease activity and increase enantiomeric excess to 52%(R). These unexpected contrary effects on activity and enantioselectivity were confirmed for Bi adsorption by repeating the experiments using the standard reference catalyst 6.3% Pt/silica (EUROPT-1), for which enantiomeric excess fell linearly from 73%(R) to 20%(R) as Bi loading was increased. The well-documented rate enhancement associated with catalyst modification by cinchonidine has been reassessed in the light of this further rate enhancement by Bi adsorption, and its origin has been attributed to inhibition of ethyl pyruvate dimerisation/polymerisation by the strongly basic alkaloid. Rate enhancement is now attributed to reaction occurring at a normal rate at an enhanced number of sites, not (as previously proposed) to a reaction occurring at an enhanced rate at a constant number of sites. The opposing effects of Bi and S on rate and enantioselectivity are consistent with (i) preferential initiation of pyruvate polymerisation at step sites, (ii) inhibition of propagation of this polymerisation by alkaloid, and (iii) a higher enantiomeric excess in cinchonidine-modified near-step sites than in similarly modified terrace sites. These results have important implications for future catalyst design.

Keywords: Enantioselective hydrogenation; Ethyl pyruvate; Bismuth; Sulfur; Surface modification; Cinchona alkaloids; Cyclic voltammetry

1. Introduction

Production of optically pure chiral compounds is of the utmost importance in the pharmaceutical, agrochemical, and fragrance industries, and much research has focused on their preparation using heterogeneous metal catalysts. Two strategies for this preparation are available: (i) enantioselective hydrogenation, in which the chiral directing agent is chemically bonded to the catalyst surface [1], and (ii) diastereoselective hydrogenation, in which the required chiral auxiliary is covalently bonded to the prochiral reactant molecule [2]. In the former, a small quantity of chiral modifier sufficient to form a partial adlayer at the metal surface is effective

* Corresponding authors.
E-mail address: attard@cf.ac.uk (G.A. Attard).

0021-9517/$ – see front matter
doi:10.1016/j.jcat.2005.06.017

and the required product is formed directly, whereas in the latter, stoichiometric quantities of chiral-directing agent are needed, and a cleavage reaction is required to provide the final product. Both methodologies when optimised can provide optical yields of 95% or more, but in general the performance of enantioselective hydrogenation catalysts has been disappointing. Their more modest performance may be due to the wide diversity of site types available at polycrystalline metal surfaces, and consequently to the generation of various enantioselective sites that differ in terms of chiral efficiency. Adsorption of the reactant in an optimal spatial relationship to the chiral environment of the adsorbed modifier is crucial to high performance, but no systematic information on the dependence of enantioselectivity on surface structure is presently available. The objective of this investigation was to explore the relationship between enantioselectivity and catalyst morphology and thereby provide a structural basis for future catalyst design. Two approaches have been adopted: (i) the selective blocking of step or terrace sites by inert adatoms and observation of the chiral performance of the remaining surface, and (ii) the variation of available site types by thermal sintering. This paper demonstrates for the first time the relationship between activity, enantioselectivity, and catalyst morphology in the enantioselective hydrogenation of ethyl pyruvate to ethyl lactate over cinchonidine-modified Pt. Sintering effects will be reported in future work.

Enantioselective hydrogenation of a range of prochiral activated ketones has been catalysed in solution by supported Pt catalysts modified by cinchona alkaloids [1]. Mechanisms have been developed that interpret not only the sense and magnitude of the enantiomeric excess, but also the variations in enantioselectivity accompanying changes in reactant, alkaloid structure, and reaction conditions [3]. With respect to catalyst morphology, early work demonstrated an inverse correlation between enantiomeric excess and platinum dispersion [4], and some investigators proposed a key role for corner atom sites in achieving enantioselectivity [5]. High values (ca. 97%) were reported for 1.4-nm colloidal Pt particles [6], again suggesting that suitable edge sites might be of importance, but 0.7-nm silica-supported Pt clusters were inactive [7], probably because of the difficulty of co-adsorbing both modifier and reactant on such restricted surfaces. Thus the potential of morphology to influence chiral outcome has been recognised, but no direct link between enantioselectivity and local surface structure has been demonstrated experimentally.

Supported metal catalysts contain polycrystalline metal particles that expose terraces, steps, and kinks (formed at step intersections) to the fluid phase. These particles have a wide size distribution and surface morphologies that depend on their size and on their chemical and thermal history. Cyclic voltammetry can provide evidence of this morphology as long as the catalyst is a conductor. Thus cyclic voltammograms (CVs) of Pt/graphite catalysts in acidic solution contain electrosorption peaks corresponding to the presence of various types of terraces and steps at the metal surface [8]. Occupation of a given type of site by an adsorbate other than hydrogen or electrolyte anion results in the partial or complete loss of that feature from the CV. Here Bi and S have been adsorbed onto Pt/graphite. Single-crystal studies have shown that Bi blocks Pt step sites in preference to {111} terrace sites, whereas S initially blocks Pt terrace {111} sites [9]. In contrast with earlier studies of chemically modified Pt surfaces, in which surface coverage of adatoms was considered the important variable determining activity and selectivity [10–13], the present investigation applies recent knowledge (gained from single-crystal Pt electrode studies in relation to the *adsorption site preference* of adatoms) to investigate the chiral efficiencies of various types of adsorption site at the molecular level. This strategy provides an opportunity to control and characterise the types of catalyst site available to reactant molecules. Whether the sites exposed during catalysis in a reactor are the same in type and number as those determined in an electrochemical cell will be determined by the normal processes of competitive adsorption that operate under reaction conditions.

The choice of Pt/graphite as the catalyst was determined by the requirement that samples for cyclic voltammetry should be conducting. We previously reported the effects of adsorption of some cinchona alkaloids on the CV of Pt/graphite [8]. Carbon- or graphite-supported Pt is generally inferior to Pt/silica and Pt/alumina in terms of chiral performance—typically Pt/C, ee = 20–45% [14,15]; Pt/silica, ee = 65–78% [16–21]; and Pt/alumina, ee = 75–85% [1,4] with special treatments such as ultrasonication [22] or particle restructuring during reaction [23] providing exceptionally high values. However, as we discuss later, detailed understanding of enantioselective surface processes that can be defined for Pt/graphite using the electrochemical surface science approach can be applied, by analogy, to nonconducting supported Pt catalysts where analogous behaviour can be established. Hence conducting Pt/graphite catalysts occupy a key strategic position in our investigation of the dependence of enantioselectivity on catalyst morphology.

The chosen enantioselective reaction involved the use of two strongly adsorbed components, ethyl pyruvate and cinchonidine. To aid interpretation of the results, we briefly report the characteristics of cyclohexene hydrogenation, a less aggressive reaction.

2. Experimental

Platinum-catalysed ethyl pyruvate hydrogenation at ambient temperature and 30-bar pressure was conducted in a stainless steel, mechanically stirred Baskerville reactor. Catalysts used were a 5% Pt/graphite (Johnson Matthey), with a Pt area of 2.1 $m^2\,g^{-1}$ and a mean Pt particle size of 14 nm, and the standard reference catalyst EUROPT-1, 6.3% Pt/silica (Johnson Matthey), with a total area of 185 $m^2\,g^{-1}$ and a mean Pt particle size of 2 nm [24,25]. Pt/graphite re-

quired no re-reduction; EUROPT-1 was re-reduced at 450 K in flowing 5% H_2 in Ar for 3 h before use.

To deposit Bi or S onto Pt/graphite or Pt/silica, 2 g samples of catalyst were immersed in predetermined volumes of aqueous 1.5 mmol bismuth nitrate solution for 3 h with vigorous stirring. The slurry was then left to stand for 18 h, filtered off, washed with 1.0 l of ultrapure water, and dried at 373 K for 0.25 h. For S deposition onto Pt/graphite, 2 g samples of catalyst were immersed in predetermined volumes of aqueous 1.5 mmol sodium sulphide solution in a bubbler, and hydrogen was passed through the solution for 0.5 h. The slurry was then sparged with nitrogen for 0.5 h, and the catalyst was filtered off, washed, and dried. Surface coverages of Bi and S on Pt/graphite were determined by cyclic voltammetry, as described later.

Pt, Pt–Bi, and Pt–S catalysts were rendered enantioselective by treatment with cinchonidine (CD) (Fluka). The quinuclidine ring system in these alkaloids is crucial to their mode of action, and hence catalyst treatment with achiral quinuclidine (QD) was also investigated. Modification (the process by which alkaloid was adsorbed onto the catalyst) was achieved in situ. Typically, 65 mmol of ethyl pyruvate (7.2 ml), 0.17 mmol of alkaloid (50 mg cinchonidine or cinchonine, 19 mg quinuclidine), 0.25 g of catalyst, and 12.5 ml of dichloromethane, in that order, were measured into the glass liner of the reactor. Once sealed, the vessel was purged several times with hydrogen to remove air, then pressurised to 30 bar. The stirrer motor was started immediately, and reaction commenced. All enantioselective reactions were allowed to proceed to 98–100% conversion. Cyclohexene hydrogenations at 5-bar pressure were conducted analogously but in the absence of alkaloid.

Reactions were carried out at constant pressure; a Buchi 9204 gas dosing system admitted hydrogen to compensate for the hydrogen consumed. Reactions over Pt/graphite and Pt/silica showed uptake-time curves of the type previously recorded for EUROPT-1 [16,17]. Reaction in the absence of an alkaloid modifier was slow, showed a decreasing rate typical of a progressively poisoned reaction, and often became immeasurably slow before complete conversion. (Activity is denoted by the initial rate, r_{initial}.) Alkaloid-modified reactions were much faster, showing an initial period of mildly accelerating rate (0 to ∼15% conversion) followed by fast reaction at constant maximum rate, $r_{\max}$ (∼15 to ∼85% conversion), and a final deceleration as the reactant became exhausted. Rates of reactions over alkaloid-modified catalysts are denoted by $(r_{\max})_{\text{CD}}$ or $(r_{\max})_{\text{QD}}$, and the rate-enhancement factor, R_{E}, is defined as $(r_{\max})_{\text{CD}}/(r_{\text{initial}})$ or $(r_{\max})_{\text{QD}}/(r_{\text{initial}})$. Cyclohexene hydrogenations showed first-order decay of reaction rate with time; activity is expressed in terms of the initial rate, r_{cyclohex}. Uncertainties in the rate measurements were generally ±1–2% of the stated values.

Products were analysed by chiral gas-liquid chromatography (25 m capillary column, chiral β-cyclodextrine stationary phase; Varian). Ethyl pyruvate hydrogenations produced mostly R- and S-ethyl lactate, with enantioselectivity quantified in terms of the enantiomeric excess, ee (%), defined as $(|[\text{R-}]-[\text{S-}]|)10^2/([\text{R-}]+[\text{S-}])$. Values of enantiomeric excess measured chromatographically for a series of synthetic standards exhibited a correlation coefficient of 0.99. A small percentage of the reactant was converted to eight high-molecular mass products (HMMPs). The total area under the HMMP peaks in each chromatogram was determined, and the value for the cinchonidine-modified reaction at 100% conversion over Bi-free Pt/graphite was given the value 100. Yields from other reactions were scaled accordingly.

The two-compartment electrochemical cell used for catalyst characterisation was as described previously [26]. The working electrode consisted of a Pt mesh basket containing 2.7 mg of Pt/graphite catalyst, the electrolyte was 0.5 mol of sulphuric acid, and the sweep rate was 10 mV s^{-1}. CVs of Pt catalysts revealed electrosorption peaks at 0.06, 0.20, 0.28, and 0.47 V attributed (in comparison with the single-crystal data) to the presence of $\{111\}_{\text{terr}} \times \{111\}_{\text{step}}$ step sites, $\{100\}_{\text{terr}} \times \{111\}_{\text{step}}$ step sites, {100} terraces, and {111} terraces, respectively [8,27,28]. The area under the voltammogram was reduced when Bi or S was adsorbed onto the Pt/graphite catalyst, and surface coverages, θ_{Bi} and θ_{S}, were calculated using the equation $\theta_{\text{Bi,S}} = [(Q_{\text{H}}^{\text{O}}) - (Q_{\text{H}}^{\text{Bi,S}})]/Q_{\text{H}}^{\text{O}}$, where $(Q_{\text{H}}^{\text{O}})$ and $(Q_{\text{H}}^{\text{Bi,S}})$ are the hydrogen sorption charges before and after adsorption of Bi or S onto the catalyst, respectively. When preparating the (Pt–Bi)/graphite catalysts, using 2.5, 5.0, 7.5, 10.0, 12.5, 15.0, 17.5, 20.0, 30.0, 40.0, and 50.0 ml bismuth nitrate solution produced Bi surface coverages (θ_{Bi}) of 0.09, 0.17, 0.26, 0.35, 0.43, 0.52, 0.70, 1.05, 1.40, and 1.70, respectively; the last two catalysts in this series contained multilayers of Bi. Likewise, (Pt–S)/graphite catalysts were prepared for which $\theta_{\text{S}} = 0.15$, 0.16, 0.19, 0.28, 0.29, 0.49. Bismuthated EUROPT-1 samples were prepared using 10.0, 20.0, 25.0, 30.0, 35.0, 40.0, and 48.0 ml bismuth nitrate solution. (Bismuth coverages could not be determined, because samples were not conducting.)

Because Bi and S coverages under reaction conditions departed from the values of θ_{Bi} and θ_{S} determined during catalyst characterisation (due to competitive adsorption effects), the coverages under reaction conditions are denoted by $(\theta_{\text{Bi}})_{\text{ch}}$ and $(\theta_{\text{S}})_{\text{ch}}$ to emphasise that these were the values determined at characterisation.

3. Results

3.1. Pt/graphite: activity and enantioselectivity

Fig. 1 shows uptake–time curves for (a) reaction over Pt/graphite in the absence of alkaloid (racemic product), (b) reaction in the presence of 0.17 mmol of the achiral modifier quinuclidine (racemic product), and (c) reaction in the presence of 0.17 mmol of the chiral modifier cinchonidine [optically active product, ee = 43%(R)]. Table 1

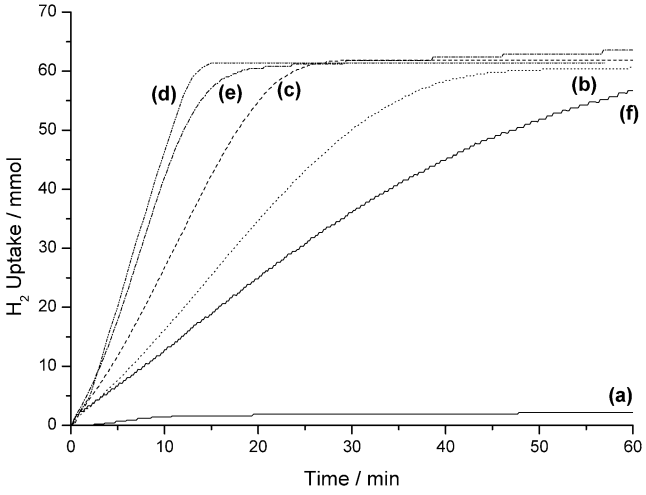

Fig. 1. Uptake/time curves for ethyl pyruvate hydrogenation at 293 K and 30 bar pressure. Catalysts: (a) unmodified Pt/graphite; (b) quinuclidine-modified Pt/graphite; (c) cinchonidine-modified Pt/graphite; (d) cinchonidine-modified Pt–Bi/graphite ($(\theta_{Bi})_{ch} = 0.43$), (e) equimolar CD:QN-modified Pt/graphite, (f) cinchonidine-modified Pt–S/graphite ($(\theta_S)_{ch} = 0.19$).

Table 1
Variation of activity (r_{max}), enantiomeric excess (ee) and HMMP yield in reactions over Pt/graphite, Pt–Bi/graphite and Pt–S/graphite modified by cinchonidine (CD) and quinuclidine (QN)[a]

Surface	Alkaloid modifier	r_{max} (mmol h^{-1} g_{cat}^{-1})	ee (%(R))	HMMP yield
Pt	None	–[b]	0	2[c]
Pt	CD	850	41	100
Pt	QN	440	0	40
Pt	1:1 CD:QN	1205	37	–
Pt–Bi ($(\theta_{Bi})_{ch} = 0.35$)	CD	1350	35	49
Pt–Bi ($(\theta_{Bi})_{ch} = 0.35$)	QN	1710	0	36
Pt–Bi ($(\theta_{Bi})_{ch} = 0.35$)	1:1 CD:QN	4600	15	–
Pt–S ($(\theta_S)_{ch} = 0.19$)	CD	440	52	109
Pt–S ($(\theta_S)_{ch} = 0.19$)	QN	310	0	–
Pt–S ($(\theta_S)_{ch} = 0.19$)	1:1 CD:QN	645	51	–

[a] Conditions: 65 mmol ethyl pyruvate, 0.17 mmol CD and/or 0.17 mmol QN, 0.25 g catalyst, 12.5 ml dichloromethane, 30 bar hydrogen, 293 K, 1000 rpm.

[b] For this reaction: $r_{initial} = 24$ mmol h^{-1} g_{cat}^{1}.

[c] Conversion, 20%.

lists the rates. The presence of cinchonidine and quinuclidine caused rate enhancements by factors (R_E) of 18 and 35, within the range of 15–50 normally observed over EUROPT-1 [4,16,29]. Using a 1:1 mixture of cinchonidine and quinuclidine (0.17 mmol of each) resulted in a previously unreported additive effect with respect to rate, with the enantiomeric excess only slightly reduced at 37%(R) (Table 1 and Fig. 1e).

3.2. Pt–Bi/graphite: characterisation

Representative CVs for the (Pt–Bi)/graphite catalysts are shown in Fig. 2. The catalyst containing no Bi showed features attributable to {111} × {111} and {100} × {111} steps

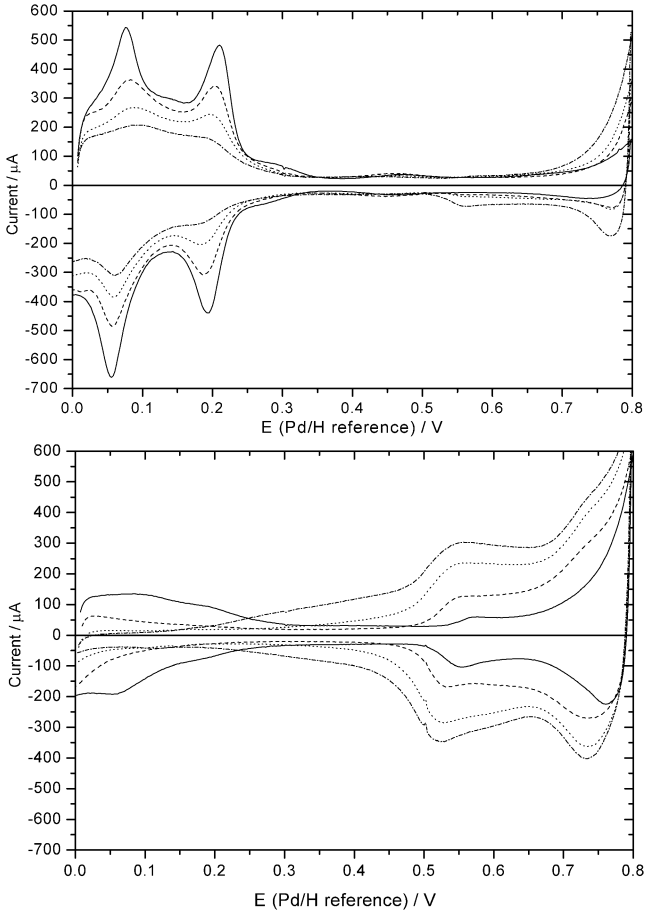

Fig. 2. CVs for Pt/graphite and bismuthated derivatives. For conditions see Experimental section. Electrosorption features: 0.06 V, {111} × {111} Pt steps; 0.20 V, {100} × {111} Pt steps; 0.28 V, {100} Pt terraces; 0.47 V, {111} Pt terraces; >0.5 V, Bi covered surface. Bismuth coverages at characterisation (top): 0.00 (full curve), 0.26 (dashed curve), 0.35 (dotted curve), 0.52 (dot-dashed curve); (bottom): 0.70 (full curve), 1.05 (dashed curve), 1.40 (dotted curve), 1.74 (dot-dashed curve).

(0.06 and 0.20 V) and to {100} and {111} terraces (0.28 and 0.47 V) (Fig. 2 (top)).

Peak shapes were consistent with the steps, demonstrating limited long-range order and narrow {111} and {100} terraces [28]. Adsorption of Bi onto this Pt surface resulted first in a diminution in the step features ($(\theta_{Bi})_{ch} = 0.09$ to 0.35), indicating that Bi was adsorbed preferentially at the step sites. Adsorption at the {100} terraces was well underway even at $(\theta_{Bi})_{ch} = 0.26$, whereas the {111} terraces were populated only at high coverages [$(\theta_{Bi})_{ch} > 0.60$]. When the bismuth loading exceeded $(\theta_{Bi})_{ch} = 0.70$, a new feature appeared at ∼0.53 V, attributable to surface redox processes associated with Bi chemisorbed at the {111} terraces (Fig. 2). The initial preferential adsorption of Bi at Pt step sites demonstrated that this morphologically complex Pt surface behaved in the manner expected from the results of Pt single-crystal studies [9,30]. Bi and S appear to be in their zero oxidation states at electrochemical potentials close to 0 V (Pd/H), although they exhibit redox behaviour under oxidising conditions (>0.9 V) [31,32]. Thus, under the re-

Table 2
Effect of bismuth coverage, $(\theta_{Bi})_{ch}$, on the rate r_{max} of ethyl pyruvate hydrogenation catalysed by Pt/graphite modified by cinchonidine (CD) or quinuclidine (QN); and the initial rate of cyclohexene hydrogenation catalysed by unmodified Pt/graphite

$(\theta_{Bi})_{ch}$	Ethyl pyruvate hydrogenation[a]		Cyclohexene hydrogenation[b]
	$(r_{max})_{CD}$	$(r_{max})_{QN}$	$r_{cyclohex}$
0.00	850	440	3670
0.09	930	640	2960
0.17	980	1095	–
0.26	1520	1440	–
0.35	1350	1710	2840
0.43	1440	2350	–
0.52	1900	1635	–
0.60	1645	1960	–
0.70	1950	–	1980
1.05	1660	–	630
1.40	1690	–	70
1.74	1755	2110	20

[a] For reaction conditions see Table 1.
[b] Reaction conditions: 100 mmol cyclohexene, 0.05 g catalyst, 20 ml dichloromethane, 5 bar dihydrogen, 293 K, 1000 rpm.

actor conditions used in this work (30-bar hydrogen), Bi and S would be expected to be present in their zero oxidation states.

3.3. Pt–Bi/graphite: activity and enantioselectivity

An uptake–time curve for cinchonidine-modified reaction over Pt–Bi/graphite [$(\theta_{Bi})_{ch} = 0.43$] is shown as curve (d) in Fig. 1. The maximum rate, $(r_{max})_{CD}$, increased with increasing Bi coverage (Table 2), with activity becoming independent of coverage for catalysts showing $(\theta_{Bi})_{ch} > 0.6$. In the presence of Bi, quinuclidine was as effective as cinchonidine in providing an enhanced rate (Table 2). Modification with 1:1 (cinchonidine + quinuclidine) mixtures produced an extremely fast reaction ($R_E = 184$, Table 1) in which the enantiomeric excess was reduced to 15%.

Rates were independent of ethyl pyruvate concentration for Pt/graphite $(\theta_{Bi})_{ch} = 0.52$ and 1.05. This indicates that the zero order in pyruvate normally reported for this reaction [16] also applied to the faster reactions at these bismuthated surfaces.

Fig. 3 shows the effect of bismuth on the enantioselectivity observed in the cinchonidine-modified reaction. Enantiomeric excess decreased with increasing bismuth coverage, with the most rapid increase occurring over the range $(\theta_{Bi})_{ch} = 0$–0.6, the region coincident with the occupation of Pt step sites by Bi in the as-prepared catalysts. The rate of decrease in the enantiomeric excess was less rapid in catalysts for which $(\theta_{Bi})_{ch} > 0.6$, that is, where bismuth adsorption occurred at the {111} terraces during preparation.

3.4. Pt–Bi/silica: activity and enantioselectivity

The effect of Bi adsorption on 6.3% Pt/silica (EUROPT-1) was similar to that on 5% Pt/graphite. The maximum rates,

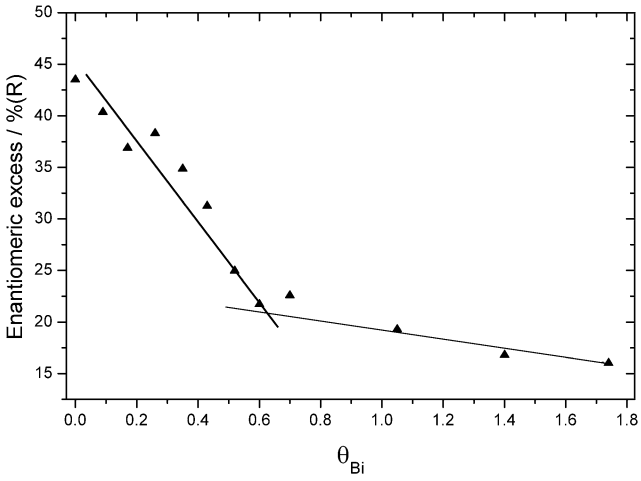

Fig. 3. Pt–Bi/graphite: variation of enantiomeric excess with bismuth coverage at characterisation. For reaction conditions see Table 1.

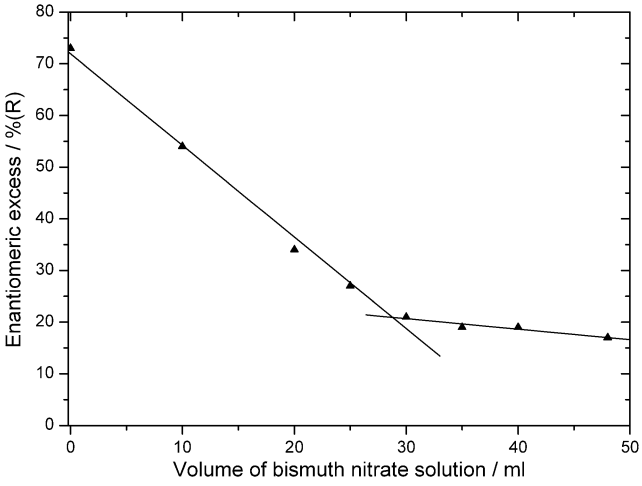

Fig. 4. Pt–Bi/silica: variation of enantiomeric excess with extent of exposure of EUROPT-1 to bismuth nitrate solution. For reaction conditions see Table 1.

$(r_{max})_{CD}$, again increased as the Bi dosage was increased (not shown), and enantiomeric excess decreased in a similar two-stage manner (Fig. 4). Although surface coverage of Bi could not be determined, we can infer that Bi occupied step sites, because the catalyst was dosed with up to 25-ml bismuth solution, and that terrace sites were occupied thereafter. Although the enantiomeric excess over Bi-free Pt/silica was 73%(R), considerably higher than that observed over Bi-free Pt/graphite, the value observed when Bi fully occupied the step sites was similar, about 20%.

3.5. Pt–S/graphite: characterisation

Fig. 5 shows CVs for clean and sulfided Pt/graphite. All features in the CV diminished as sulfur was progressively adsorbed; the {100} terrace feature (0.25 V) was most rapidly attenuated, and the {111} terrace feature (0.46 V) was lost by $(\theta_S)_{ch} = 0.28$, leaving only the step features

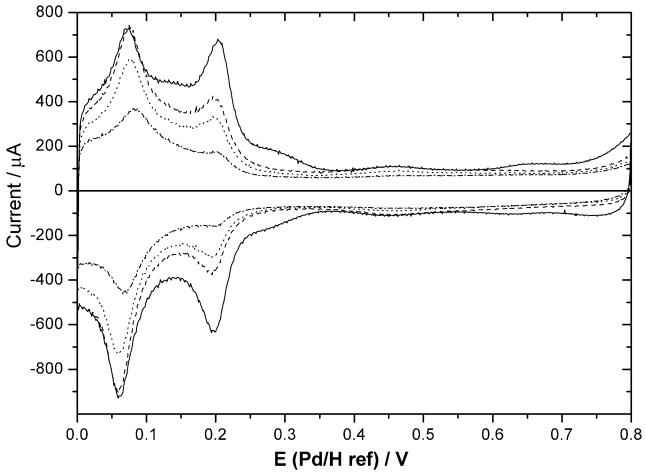

Fig. 5. CVs for Pt/graphite and sulfided derivatives. For conditions see Experimental section. Sulfur coverages at characterisation: 0.00 (full curve), 0.16 (dashed curve), 0.28 (dotted curve), 0.49 (dot-dashed curve).

Table 3
Effect of sulfur coverage as determined during characterisation, $(\theta_S)_{ch}$, on the rate of hydrogenation, $(r_{max})_{CD}$, and enantiomeric excess, ee, for ethyl pyruvate hydrogenation catalysed by cinchonidine-modified Pt/graphite; and the initial rate, $r_{cyclohex}$, of cyclohexene hydrogenation catalysed by unmodified Pt/graphite

$(\theta_S)_{ch}$	Ethyl pyruvate hydrogenation[a]		Cyclohexene hydrogenation[a]
	$(r_{max})_{CD}$ (mmol h^{-1} g^{-1})	ee (%)	$r_{cyclohex}$ (mmol h^{-1} g^{-1})
0.00	860	42.2	3640
0.15	360	54.0	–
0.16	360	51.4	–
0.19	440	51.6	–
0.28	280	51.0	2760
0.29	–	–	2700
0.49	270	53.5	2120
0.55	–	–	1950

[a] For reaction conditions see Table 1.

present, of which the {111} × {111} step sites were most prominent. Thus S exhibited preferential adsorption at the terrace sites, although its selectivity toward adsorption at these sites was not as high as that of Bi toward step sites. Of the step sites, the {100} × {111} steps were occupied in preference to the {111} × {111} steps in the earliest stages of S adsorption. Coverages beyond $(\theta_S)_{ch} \approx 0.5$ could not be achieved using this preparation technique.

3.6. Pt–S/graphite: activity and enantioselectivity

Table 3 shows that activity for cinchonidine-modified reaction declined as S-coverage increased, whereas enantiomeric excess increased from 42%(R) for S-free Pt/graphite to 51–54%(R) for the sulfided catalysts ($(\theta_S)_{ch} = 0.15$–0.49).

3.7. HMMPs

HMMP yields are given in Table 1. The yield in cinchonidine-modified pyruvate hydrogenation at 100% conversion over Bi-free Pt/graphite was given the value of 100, and values for other reactions were scaled accordingly (see Experimental section). Yields were lower in the faster Pt–Bi-catalysed reactions and higher in the slower Pt–S-catalysed reactions.

Reactions over untreated Pt/graphite (with Bi, S, and alkaloid absent) became immeasurably slow at modest conversions. The relative HMMP yield at 20% conversion was 2.

Four major components constituted more than 90% of the HMMP yield and were found to have mass 234 on mass spectrometry: the four diastereoisomers of (I), which is termed "adduct-(I)" because it may be considered an adduct of ethyl pyruvate and ethyl lactate.

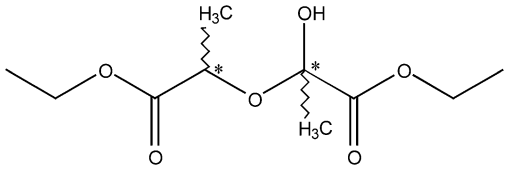

adduct-(I)

Two minor products of mass 232 (Scheme 1) seen only in racemic reactions in the absence of alkaloid, Bi, and S, were the enantiomers of pyruvate ester dimer (II). Both adduct-(I) (a diester) and dimer-(II) (an α-ketoester) may have reacted further with ethyl pyruvate to form higher polymers on the surface that were not detected. The mechanism proposed in Scheme 1 differs from the aldol-type reaction with alkanol elimination reported previously [33,34], which is inconsistent with the present mass measurements. The enol reacted with the alpha-keto group, not with the ester carbonyl. The processes in Scheme 1 are expected to be reversible and the equilibria will be responsive to the presence of acids and bases, including the modifier alkaloid. Thus the absence of dimer-(II) among the HMMPs formed in the presence of alkaloid is interpreted as being due to inhibition of its formation by alkaloid in alkaloid-modified reactions.

3.8. Cyclohexene hydrogenation

Initial rates for cyclohexene hydrogenation over Pt/graphite ($r_{cyclohex}$) are reported in Tables 2 and 3. With increasing $(\theta_{Bi})_{ch}$, activity fell to 54% of its original value at $(\theta_{Bi})_{ch} = 0.70$, and to 17% at $(\theta_{Bi})_{ch} = 1.05$. Because the CVs indicated full surface coverage of the Pt surface by Bi at $(\theta_{Bi})_{ch} = 1.07$, cyclohexene hydrogenation clearly caused some displacement of Bi and the reemergence of active Pt surface. With increasing S coverage, activity for cyclohexene hydrogenation dropped by 45% at $(\theta_S)_{ch} = 0.55$, confirming that considerable Pt surface remained exposed both in the as-prepared catalyst and under reaction conditions. Because pyruvate ester and cinchonidine are more strongly adsorbed than cyclohexene, we would expect them to cause greater displacement of Bi from the active surface.

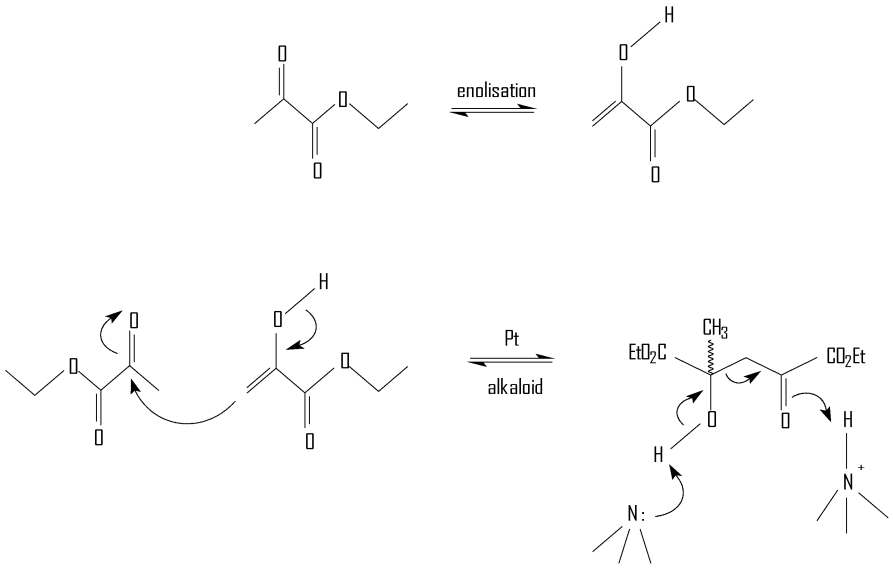

Scheme 1.

4. Discussion

4.1. Surface conditions

The adsorption of cationic Bi and anionic S onto Pt/graphite proceeded in a fashion similar to that observed for the same adsorbates on Pt single crystals [9]. Steps at a Pt surface exhibit a dipole moment [9]. Bi, being more electropositive than Pt, is attracted to the steps [9], whereas S, being more electronegative, is repelled from the steps onto adjacent terraces [9]. Electronegativity differences imply that the Pt–Bi and Pt–S bonds have partial ionic character, as has been confirmed by work function measurements [35,36]. However (as indicated earlier), CV indicated that Bi and S were in their zero oxidation states at 0 V, and hence the results are discussed in terms of a simple geometric site-blocking model. We will shortly be starting an X-ray spectroscopy study to determine the extent of any electronic effects of Bi and S on Pt/graphite. Using sodium sulphide as the source of S may have led to the presence of some residual sodium in Pt–S/graphite catalysts despite the stringent washing procedure used during preparation. We consider any effect of residual sodium unimportant in light of the zero/marginal effect of adding potassium ion to catalysts for this reaction (data not published).

4.2. Mechanistic models

Two types of mechanisms have been advanced to interpret the enantioselective hydrogenation of pyruvate esters catalysed by cinchonidine-modified supported Pt. The *adsorption model* proposes that each alkaloid molecule adsorbed at the Pt surface in the open-3 conformation creates a chiral environment in its vicinity at which pyruvate ester can undergo selective enantioface adsorption [4,19]. In this model, cinchonidine is π-adsorbed by the quinoline moiety [37,38] and pyruvate ester is π-adsorbed by both carbonyl functions. Optically active product is then formed on hydrogenation. Such enantioselective sites each require 25 or so Pt atoms to achieve simultaneous adsorption of modifier, reactant, and hydrogen [19]. The *chemical shielding model* proposes that the alkaloid in a closed conformation forms a shielded complex with pyruvate ester such that on adsorption, hydrogen atoms can be added to only one face of the ester molecule, thereby forming an optically active product [39–43]. Both of these models predict the sense of the observed enantioselectivity (i.e., preferential R-lactate formation in the presence of cinchonidine, preferential S-lactate formation in the presence of cinchonine). The adsorption model commands greater support because (i) the conformational characteristics of cinchonidine in solution are known from nuclear magnetic resonance spectroscopy [44,45] and (provided that the conformational balance observed in solution is assumed to be largely retained on adsorption) the conditions that favour the open-3 conformation are those that favour high enantioselectivity [46]; (ii) cinchonidine derivatives braced in the open conformation also yield preferential R-product formation [47]; (iii) substituted cinchonidines yield increases or decreases in enantiomeric excess under standard conditions for which structural intepretations have been advanced [4]; and (iv) synthetic analogues of simpler structure but retaining the same functional entities are effective modifiers [48–51]. The discussion here is based on the adsorption model.

4.3. Reactions over Pt/graphite

Cinchonidine-modified reactions over Pt/graphite showed low rates in the absence of alkaloid, enhanced rates in the

presence of alkaloid, and an enantiomeric excess in favour of R-lactate (Fig. 1 and Table 1). Pt/graphite behaved like Pt/silica and Pt/alumina in these respects, except that the enantiomeric excess at ∼45%(R) was lower than the values of ∼75%(R) given by oxide-supported Pt without optimisation under the same conditions [1,4]. A value of 45% over Pt/(amorphous-C) was also obtained by Orito et al. [14] in their original studies of this reaction; lower values have been reported for a range of other Pt/C catalysts [15].

Fig. 1 and Table 1 show that quinuclidine enhanced rate by a factor of 18, so that racemic reaction proceeded rapidly to completion. We have previously reported that simple amines accelerate reaction to an extent depending on their basicity [29]. The effect was interpreted in terms of H-bonding between the N-atom of modifier molecules in solution and adsorbed σ-bonded half-hydrogenated states of the type MeC(OH)COOR(ads), which were thereby stabilised and their surface coverage (and hence the reaction rate) enhanced. Cinchonidine enhanced the rate by a factor of 35, again as expected on this basis. Modification with a 1:1-mixture of cinchonidine and quinuclidine yielded $R_E = 52$, which was additive, as expected, but the enantiomeric excess was only slightly depressed. Thus the presence of *achiral* quinuclidine resulted in the more-rapid formation of *chiral* product.

This unexpected observation has necessitated a revision of our rate-enhancement mechanism. Scanning tunnelling microscopy (STM) has recently provided direct evidence that ethyl pyruvate polymerises at the Pt{111} surface [52] and that in the absence of hydrogen, individual polymer chains nucleate from defect sites. In the presence of hydrogen, monomers decorate step edges. This finding confirms our long-held suspicion, based on the kinetics and HMMP formation, that pyruvate ester polymerisation is the most likely cause of the slow rate of racemic reaction over supported Pt catalysts in the absence of a N-base. Because the surface oligomeric species proposed here are formed reversibly, the effect of N-bases is to decouple dimer-(II) by the reverse of Scheme 1, reforming ethyl pyruvate monomer and, if adduct-(I) can undergo hydrogenolysis, forming ethyl lactate. Thus, in the dynamic situation of polymer initiation, propagation, and decoupling, the overall effect of N-bases on dimer-(II) formation is one of general inhibition. Pt surface formerly poisoned by polymer is thereby released for productive hydrogenation of ethyl pyruvate. On this basis, rate enhancement is due to reaction occurring at normal rate at an increased number of sites and not, as formerly supposed, due to reaction occurring at enhanced rate at a constant number of sites. Thus, when both cinchonidine and quinuclidine were present, they acted cooperatively in decoupling the pyruvate ester polymer and increased the fraction of productive surface. Cinchonidine, being much more strongly adsorbed than quinuclidine, was then able to adsorb preferentially on the newly released Pt surface, and hence most of the faster pyruvate hydrogenation resulted in chiral product and enantiomeric excess was maintained largely at 37%.

Alkaloid had opposite effects on the two processes of HMMP formation. Dimer-(II) was formed mostly at the Pt surface but was decoupled by N-base, as discussed earlier, and any higher polymers would be expected to be similarly decoupled. In contrast, adduct-(I) was formed in a higher yield in the presence of N-bases (Table 1), indicating that its formation was base-catalysed. Note that dimer-(II) is also formed when cinchonidine and ethyl pyruvate are left to stand in dichloromethane, so there was a subsidiary source of dimer-(II) from a homogeneous process in all of these catalytic reactions.

This model predicts unexpected behaviour with respect to both rate and enantiomeric excess toward the end of reaction when the residual concentration of pyruvate in solution becomes small. As the concentration of pyruvate ester diminishes, the equilibria shown in Scheme 1 will shift to favour the monomer, and dimer-(II) will undergo desorption, leading to an increase in available Pt surface, particularly edge sites. Thus there should be an increase in both rate and enantiomeric excess. Results tending to confirm these expectations have been published elsewhere [53]. Clearly, mass transport of dimer-(II) both within the solution and to and from the Pt surface is an important factor in determining the poisoning effects of HMMPs on the overall reaction.

4.4. Reactions over Pt–Bi/graphite

Pt/graphite catalysts, which at characterisation exhibited progressive preferential adsorption of Bi at Pt step sites (Fig. 2), showed a progressive increase in rate and decrease in enantiomeric excess for cinchonidine-modified reactions (Table 2 and Fig. 3) and an increase in rate for racemic quinuclidine-modified reactions. This behaviour contrasts directly with the sympathetic change in activity and enantioselectivity normally observed and establishes that rate enhancement and achievement of an enantiomeric excess are separate phenomena within this reaction. The decrease in enantiomeric excess as a function of Bi coverage of defect sites demonstrates that enantioselective sites at or near a step were more effective (i.e., produced a higher enantiomeric excess) than enantioselective sites on terraces away from a step. The rate enhancements that accompanied step site occupation by Bi [e.g., $R_E \approx 80$ at $(\theta_{Bi})_{ch} = 0.7$] show that (i) polymer/dimer-(II) formation was initiated preferentially at step sites (supported by STM data [52]) and (ii) a much greater degree of Bi displacement occurred than was the case with cyclohexene hydrogenation. In this model, as Bi coverage increased, the rate of polymer/dimer-(II) formation decreased, polymer/dimer-(II) decoupling by cinchonidine or quinuclidine remained efficient, but yet more Pt surface was available for ethyl pyruvate hydrogenation. Co-modification with cinchonidine and quinuclidine again gave an additive rate enhancement [$R_E = 180$ at $(\theta_{Bi})_{ch} = 0.35$ (Table 1), the highest value recorded], but because most of this faster reaction was catalysed at terraces that yielded lower enantiose-

lectivity, the value of the enantiomeric excess was typical of that for terrace reaction (i.e., 15%).

In this new model of rate enhancement, dimer-(II) plays a key role, predicated by the monomer's ability to react in its enol form. Thus it should follow that comparable reactants that cannot enolise should not provide enhanced rates in the presence of N-bases. The literature reports that ethylbenzoyl formate (PhCOCOOEt) and ketopantolactone are enantioselectively hydrogenated over cinchonidine-modified Pt at rates only slightly exceeding those of the respective racemic hydrogenations in the absence of alkaloid [54–56]. The decline in the yields of the four diastereoisomers of adduct-(I) with increasing $\theta_{Bi(ch)}$ (Table 1) indicates that these products, like dimer-(II), were formed at step sites, the availability of which was progressively reduced as bismuth coverage was increased.

4.5. Reactions over Pt–S/graphite

Catalysts that demonstrated progressive preferential adsorption of S at Pt terrace sites at characterisation (Fig. 3) exhibited a progressive diminution of rate but an immediate increase in enantiomeric excess from 42 to 51–54% that was independent of S coverage (Table 1). Because the step sites were not efficiently blocked by S, the rate of dimer-(II)/polymer formation was not markedly reduced. Hence the same degree of surface poisoning by polymer occurred in each reaction, mitigated only by the rate enhancement due to polymer decoupling by the modifier, and the overall rate diminished because adsorbed S reduced the total number of Pt sites available. Equimolar mixtures of cinchonidine and quinuclidine had an additive effect on the rate, as expected, but because only step sites remained exposed at $(\theta_S)_{ch} = 0.28$–0.45, all reaction was occurring at the most enantioselective sites, and hence the enantiomeric excess was invariant with S coverage over this range. This leads to the surprising conclusion that ee = 54% (i.e., 77% R-lactate, 23% S-lactate) is the highest enantioselectivity that graphite-supported Pt particles of this particular size distribution and surface morphology can provide. Clearly, Pt/silica and Pt/alumina, having different size distributions and morphologies, perform better. We will test these conclusions in future work when we report the sintering of Pt/graphite and its effect on particle morphology and enantioselectivity [57].

5. Conclusions

For Pt/graphite, enantioselective sites in the region of surface steps provide a mean enantiomeric excess of ∼54%(R), whereas sites on terraces more remote from steps yield a mean value of ∼17%(R). For Pt/silica, sites in the region of surface steps show higher values of enantiomeric excess [>75%(R)], with terrace sites exhibiting ∼20%(R). The influences of support and particle morphology on enantiomeric excess indicate not only that enantioselectivity varies over the surface of a given Pt nanoparticle, but also that edge sites provide the highest enantioselectivity. This may also be associated with the recent reports of enhanced enantiomeric excess occurring after sonication [22] and resulting from particle reconstruction during reaction [23], given that such processes may create new edge sites.

Rate enhancement in the presence of an alkaloid modifier is attributed to the inhibition of pyruvate ester polymerisation at the Pt surface and results from reaction occurring at a normal rate at an increased number of sites, not (as was once thought) to reaction occurring at an enhanced rate at a constant number of sites. Exceptions to the widely reported synergy between rate and enantioselectivity can now be accommodated by the proposed mechanism. HMMPs provide evidence of the participation of enolic forms of ethyl pyruvate in reactions at these surfaces.

Acknowledgments

Support was provided by the EPSRC and Johnson Matthey (to D.J.J.) and the Saudi Arabian Government (to A.M.S.A.).

References

[1] M. Studer, H.-U. Blaser, C. Exner, Adv. Syn. Catal. 45 (2003).
[2] P. Kekula, R. Prins, Top. Catal. 25 (2003) 29.
[3] P.B. Wells, R.P.K. Wells, in: D.E. De Vos, I.F.J. Vankelecom, P.A. Jacobs (Eds.), Chiral Catalyst Immobilisation and Recycling, Wiley–VCH, Weimheim, 2000, pp. 123–154.
[4] J.T. Wehrli, A. Baiker, D.M. Monti, H.-U. Blaser, J. Mol. Catal. 61 (1990) 207.
[5] R.L. Augustine, S.K. Tanielyan, L.K. Doyle, Tetrahedron: Asymmetry 4 (1993) 1803.
[6] X.I. Zuo, H. Liu, M. Liu, Tetrahedron Lett. 39 (1998) 1941.
[7] S.D. Jackson, M.B.T. Keegan, G.D. McLellan, P.A. Meheux, R.B. Moyes, G. Webb, P.B. Wells, R. Whyman, J. Willis, in: V.G. Poncelet, et al. (Eds.), Preparation and Characterisation of Catalysts, vol. V, Elsevier, Amsterdam, 1991, p. 135.
[8] G.A. Attard, J.E. Gillies, C.A. Harris, D.J. Jenkins, P. Johnston, M.A. Price, D.J. Watson, P.B. Wells, Appl. Catal. A 222 (2001) 393.
[9] E. Herrero, V. Climent, J.M. Feliu, Electrochem. Commun. 2 (2000) 636.
[10] T. Mallat, S. Szabo, M. Schurch, U.W. Gobel, A. Baiker, Catal. Lett. 47 (1997) 221.
[11] Z. Bodnar, T. Mallat, I. Bakos, S. Szabo, Z. Zsoldos, Z Schay, Appl. Catal. A 102 (1993) 105.
[12] S. Szabo, Int. Rev. Phys. Chem. 10 (1991) 207.
[13] S. Szabo, I. Bakos, J. Electroanal. Chem. 492 (2000) 103.
[14] Y. Orito, S. Imai, S. Niwa, Nippon Kagaku Kaishi (1979) 1118.
[15] M.A. Fraga, M. Meules, E.J. Jordao, J. Mol. Catal. A: Chem. 179 (2002) 179, 243.
[16] I.M. Sutherland, A. Ibbotson, R.B. Moyes, P.B. Wells, J. Catal. 125 (1990) 77.
[17] P.A. Meheux, A. Ibbotson, P.B. Wells, J. Catal. 128 (1991) 387.
[18] J.A. Slipszenko, S.P. Griffiths, P. Johnston, K.E. Simons, W.A.H. Vermeer, P.B. Wells, J. Catal. 179 (1998) 267.
[19] K.E. Simons, P.A. Meheux, S.P. Griffiths, I.M. Sutherland, P. Johnston, P.B. Wells, A.F. Carley, M.K. Rajumon, M.W. Roberts, A. Ibbotson, Recl. Trav. Chim. Pays-Bas 113 (1994) 465.

[20] P.B. Wells, K.E. Simons, J.A. Slipszenko, S.P. Griffiths, D.F. Ewing, J. Mol. Catal. A: Chem. 146 (1999) 159.
[21] S.P. Griffiths, P. Johnston, P.B. Wells, Appl. Catal. 191 (2000) 193.
[22] B. Toeroek, K. Balazsik, M. Toeroek, K. Felfoeldi, M. Bartok, Catal. Lett. 81 (2002) 55.
[23] R. Hess, F. Krumeich, T. Mallat, A. Baiker, Catal. Lett. 92 (2004) 141.
[24] G.C. Bond, P.B. Wells, Appl. Catal. 18 (1985) 225.
[25] J.W. Geus, P.B. Wells, Appl. Catal. 18 (1985) 231, and following papers.
[26] R.W. Evans, G.A. Attard, J. Electroanal. Chem. 345 (1993) 337.
[27] G.A. Attard, A. Ahmadi, D.J. Jenkins, O.A. Hazzazi, P.B. Wells, K.G. Griffin, P. Johnston, J.E. Gillies, Chem. Phys. Chem. 4 (2003) 123.
[28] J. Clavilier, K. El Achi, A. Rodes, Chem. Phys. 141 (1990) 1.
[29] G. Bond, P.A. Meheux, A. Ibbotson, P.B. Wells, Catal. Today 10 (1991) 371.
[30] O.A. Hazzazi, PhD thesis, Cardiff University, 2002.
[31] S.G. Sun, S.P. Chen, N.H. Li, G.Q. Lu, B.Z. Chen, F.C. Xu, Colloids Surf. A 134 (1998) 207.
[32] G. Wittstock, A. Strubing, R. Szargan, G. Werner, J. Electroanal. Chem. 444 (1998) 61.
[33] M. Bartok, P. Szabo, T. Bartok, G. Szollosi, Rapid Commun. Mass Spectrom. 14 (2000) 509.
[34] D. Ferri, T. Burgi, K. Borszeky, T. Mallat, A. Baiker, J. Catal. 193 (2000) 139.
[35] M.T. Paffett, C.T. Campbell, T.N. Taylor, J. Chem. Phys. 85 (1986) 6176.
[36] H. Gutleben, E. Bechtold, Surf. Sci. 191 (1987) 157.
[37] T. Evans, A.P. Woodhead, A. Gutierrez-Sossa, G. Thornton, T.J. Hall, A.A. Davis, N.A. Young, P.B. Wells, R.J. Oldman, O. Plashkevych, O.H. Vahtras, H. Agren, V. Carravetta, Surf. Sci. 436 (1999) L2167.
[38] G. Bond, P.B. Wells, J. Catal. 150 (1994) 329.
[39] J.L. Margitfalvi, M. Hegedus, E. Tfirst, Tetrahedron: Asymmetry 7 (1996) 571.
[40] J.L. Margitfalvi, M. Hegedus, E. Tfirst, Stud. Surf. Sci. Catal. 101 (1996) 241.
[41] J.L. Margitfalvi, M. Hegedus, J. Mol. Catal. A: Chem. 107 (1996) 281.
[42] J.L. Margitfalvi, E. Tfirst, J. Mol. Catal. A: Chem. 134 (1999) 81.
[43] J.L. Margitfalvi, E. Talas, E. Tfirst, C.V. Kumar, A. Gergely, Appl. Catal. 191 (2000) 177.
[44] G.D.H. Dijkstra, R.M. Kellogg, H. Wynberg, J.S. Svendsen, I. Marko, K.B. Sharpless, J. Am. Chem. Soc. 111 (1989) 8070.
[45] G.D.H. Dijkstra, R.M. Kellogg, H. Wynberg, J. Org. Chem. 55 (1990) 6121.
[46] T. Burgi, A. Baiker, J. Am. Chem. Soc. 120 (1998) 12920.
[47] M. Bartok, K. Felfoldi, G. Szollosi, T. Bartok, Catal. Lett. 6 (1999) 1.
[48] G. Wang, T. Heinz, A. Pfaltz, B. Minder, T. Mallat, A. Baiker, J. Chem. Soc. Chem. Commun. (1994) 2047.
[49] K.E. Simons, G. Wang, T. Heinz, A. Pfaltz, A. Baiker, Tetrahedron: Asymmetry 6 (1995) 505.
[50] B. Minder, T. Mallat, A. Baiker, G. Wang, T. Heinz, A. Pfaltz, J. Catal. 154 (1995) 371.
[51] A. Baiker, in: D.E. De Vos, I.F.J. Vankelecom, P.A. Jacobs (Eds.), Chiral Catalyst Immobilisation and Recycling, Wiley–VCH, Weinheim, 2000, p. 155.
[52] J.M. Bonello, R.M. Lambert, N. Kunzle, A. Baiker, J. Am. Chem. Soc. 122 (2000) 9864.
[53] D.G. Blackmond, J. Catal. 176 (1998) 267.
[54] M. Sutyinszki, K. Szori, K. Felfoldi, M. Bartok, Catal. Lett. 81 (2002) 281.
[55] M. Schurch, O. Schwalm, T. Mallat, J. Weber, A. Baiker, J. Catal. 169 (1996) 275.
[56] M. Schurch, N. Kunzle, T. Mallat, A. Baiker, J. Catal. 176 (1998) 569.
[57] D.J. Jenkins, PhD thesis, Cardiff University, 2003.